ELSEVIER

Solid State Ionics 149 (2002) 217–226

SOLID STATE IONICS

www.elsevier.com/locate/ssi

In search of the cubic phase of the Li^+ ion-conducting perovskite $La_{2/3-x}Li_{3x}TiO_3$: structure and properties of quenched and in situ heated samples

Odile Bohnke [a,*], Huguette Duroy [a], Jean-Louis Fourquet [a], Silvia Ronchetti [b], Daniele Mazza [b]

[a] *Laboratoire des Fluorures (UMR CNRS 6010), Faculté des Sciences et des Techniques, Université du Maine, Avenue Olivier Messiaen, 72085 Le Mans Cedex 9, France*

[b] *Dipartimento di Scienza dei Materiali, Politecnico di Torino, 10129 Turin, Italy*

Received 6 July 2001; received in revised form 28 February 2002; accepted 8 March 2002

Abstract

In search of the cubic phase of the Li^+ ion-conducting perovskite $La_{2/3-x}Li_{3x}TiO_3$ (LLTO), several samples, quenched and heated at different temperatures, are examined by powder X-ray diffraction (XRD). The best structural model (for $0.06 < x < 0.14$)—probably representing an average situation—is discussed in comparison with various other structural studies. It presents a tetragonal unit cell (space group $P4/mmm$; $a \approx a_p$, $c \approx 2a_p$) in which La^{3+} ions and vacancies are always unequally distributed in the two different A sites, centers of the perovskite dodecahedral cages. The quenching experiments bring the evidence of a very fast disordering/ordering of La^{3+} ions between their two unequivalent positions, and the in situ thermodiffractometry experiments show that the La^{3+} ion thermal diffusion becomes noticeable above 800 °C and depends on the solid solution composition x. Although the thermal diffusion of the La^{3+} ions occurs above 800 °C, the disordering of these ions remains limited for low x values (with $c/2a$ values slightly greater than 1) even at 1200 °C, while a nearly complete disordering is reached at 1200 °C for $x = 0.11$ (with $c/2a$ very close to 1). As reported by earlier authors, the kinetics of the fast La^{3+} ions disordering/ordering in the temperature range 900–1200 °C has to be fully considered during the preparation of the samples, and the thermal history can noticeably change the La^{3+} ion partition and hence the electrical conductivity of the prepared phase. The equilibrated samples can be obtained by using proper heating time and temperature.

Keywords: Lithium lanthanum titanate; Quenched samples; High temperature X-ray powder diffraction; La^{3+} ions ordering/disordering

1. Introduction

The $La_{2/3-x}Li_{3x}TiO_3$ solid solution (LLTO) is probably up to now the best Li^+ ionic conductor ($\sigma \approx 10^{-3}$ S cm^{-1} at RT for $x \approx 0.11$) [1–3]. Many papers have been devoted to this material both in terms of crystallographic structure and physical properties [4–35]. However, some points still remain controversial, particularly, in our opinion, the existence of the cubic phase.

Various unit cells derived from the perovskite (cell parameter a_p) were proposed by different authors.

* Corresponding author. Tel.: +33-2-43-83-33-54; fax: +33-2-43-83-35-06.

E-mail address: odile.bohnke@univ-lemans.fr (O. Bohnke).

0167-2738/02/$ - see front matter
PII: S0167-2738(02)00142-X

Kawai and Kuwano [3] were the first to report the cell parameters of the solid solution compounds and the occurrence of the tetragonal distortion from the cubic perovskite subcell at $x < \sim 0.1$. Afterwards, Robertson et al. [4] studied the phase diagram, where they have shown that a pure phase exists in the composition domain $0.06 < x < 0.14$, and they claimed the existence of two different tetragonal unit cells and of a cubic phase at high temperature. On the basis of powder X-ray diffraction (XRD) and Transmission Electron Microscopy (TEM), Fourquet et al. [5] proposed a tetragonal symmetry ($P4/mmm$) with $a = a_p$ and $c \approx 2a_p$. They clearly showed that the $c/2a$ distortion vanishes suddenly near $x = 0.08$, as previously reported by Kawai and Kuwano [3]. These authors showed that the width and the intensity of the superstructure lines become broader and less intense as the Li content increases. This was explained by the unequal distribution of the La^{3+} ions over the two A sites of the structure and the presence of antiphase domains that creates a disorder. Later, Ibarra et al. [6] extended the pure phase domain to $0.03 < x < 0.167$ by increasing the synthesis temperature. They showed that a change of symmetry occurs as lithium content increases. They proposed an orthorhombic symmetry ($Pmmm$) with $a \approx a_p$, $b \approx a_p$ and $c \approx 2a_p$ for low lithium content ($x < 0.0625$) and a tetragonal symmetry for higher lithium content. Varez et al. [7] claimed the existence of a tetragonal mutiple cell ($a = a_p \sqrt{2}$, $c \approx 2a_p$). Their assumption is based on the observation of very few and faint diffraction lines (e.g. $d_{hkl} = 2.3$ Å). Recently, Alonso et al. [8] proposed a rhombohedral symmetry ($R\bar{3}c$) for $x = 0.167$ ($La_{0.5}Li_{0.5}TiO_3$). This paper is based on a neutron powder diffraction study. However, this solution does not seem very convincing because this model does not generate the lines, which we call hereafter the superstructure lines, on the experimental X-ray diffraction (XRD) or neutron diffraction patterns, whatever the composition and the quenching temperature may be. At the microscopic level, the studies performed on many samples by Transmission Electron Microscopy (TEM) and High Resolution Electron Microscopy (HREM) revealed a severe multitwinned situation leading to an apparent cubic cell with $a \approx 2a_p$ [5,7]. Nevertheless, most of these authors agree with the fact that LLTO consists of a doubled perovskite unit cell.

Independently of the probable existence of a larger cell due to a very slight tilting of the TiO_6 octahedra, it seems however that the tetragonal unit cell ($a = a_p$ and $c \approx 2a_p$, SP = $P4/mmm$) could be used to approach the true equilibrium structure and it will be used in this paper. Table 1 shows the retained atomic model. It is derived from the study of Abe and Uchino [36] on $La_{2/3}TiO_{3-\delta}$ and is characterized by an unequal distribution of both vacancies and La^{3+} ions in the perovskite cages along the c-axis (La1 and La2 positions). Fig. 1 shows a schematic view of LLTO based on the $P4/mmm$ structural model. According to this model, the La^{3+} ions are centered in the A-cage of the perovskite structure formed by eight TiO_6 octahedra. On the other hand, if the La^{3+} ion location is perfectly defined, the location of the Li^+ ions has been a matter of debate. In a previous paper [37], by using the concept of valence sum calculation developed by Brese and O'Keeffe [38], we have shown that the Li^+ ions spread over several crystallographic positions inside the A-cage of the perovskite structure and avoid the centre of the cage. This seems realistic if we consider the small radius of this ion and the size of the cage.

Apart from the position of the La^{3+} ion in the A-cage, we are also concerned about the distribution of this species between the two positions (La1 and La2) of the perovskite A-cages in the c-direction. Indeed, an unequal distribution (or ordering of these ions) in La1 and La2 leads to the presence of the superstructure lines observed on the XRD patterns (the superstructure lines correspond to the [hkl] planes with $l = 2n + 1$). The presence of these superstructure lines implies the doubling of the perovskite cell parameter in the c-direction. If complete La^{3+} disordering can occur, a cubic perovskite LLTO would form as claimed by some authors that obtained this phase after quenching

Table 1
Structural model for LLTO (space group $P4/mmm$)

Atom	Position	Atomic coordinates
La1 + □	1a	0, 0, 0
La2 + □	1b	0, 0, 1/2
Ti	2h	1/2, 1/2, $z \approx 0.25$
O1	1c	1/2, 1/2, 0
O2	1d	1/2, 1/2, 1/2
O3	4i	0, 1/2, $z \approx 0.25$

□ = vacancies.

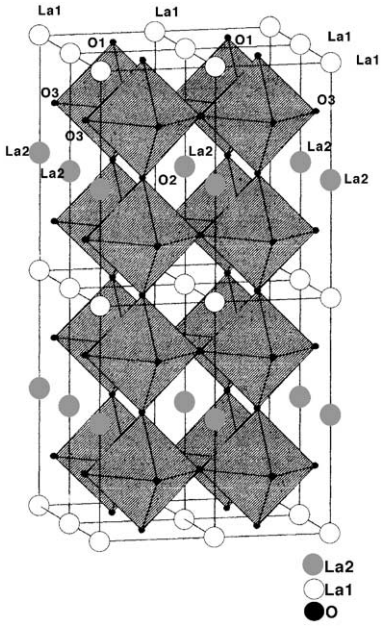

Fig. 1. Structural model for $La_{2/3-x}Li_{3x}TiO_3$ (space group *P*4/*mmm*).

[4,6,9–12]. As a consequence of the equal distribution of La^{3+} ions between La1 and La2, the superstructure lines would disappear. However, a careful examination of most of the published XRD patterns of the quenched samples continues to reveal very broad but still present superstructure lines [6,9–11].

In this paper, we present and discuss the results of powder XRD experiments performed on quenched samples for two compositions, $x=0.09$ and $x=0.11$. We also performed in situ high temperature X-ray diffractometry on both low ($x=0.06$) and high ($x=0.11$) Li^+-containing samples. A careful study of the powder XRD patterns is carried out. The results concerning the absence of superstructure lines after quenching are at variance with what has been proposed by previous authors.

2. Experimental

2.1. Preparation of the samples for quenching experiments

(a) Samples were prepared in platinum boats by conventional solid-state reactions from stoichiometric amounts of commercial products: TiO_2 (99.5%), Li_2CO_3 (99.99%) and freshly dehydrated La_2O_3 (99.999%). The starting materials were mixed and pressed into pellets. They were first heated at 850 °C for 4 h and held at 1050 °C for 12 h. After grinding and pressing, the samples were heated two times for 12 h at 1100 and 1150 °C, respectively. These heating treatments were followed by a natural cooling step in the furnace. The composition $x=0.11$ was then synthetized. As described in a previous paper [5], the chemical analysis of the sample revealed that this procedure does not lead to Li_2O loss. After quenching, they were characterized by powder XRD.

(b) Another set of samples, used for conductivity measurements after quenching, has been prepared. In order to minimize the grain boundary contribution to the electrical conductivity, these samples were prepared as follows: the starting materials were mixed and pressed into pellets; they were first heated at 850 °C for 4 h and held at 1050 °C for 12 h. After grinding and pressing, the samples were heated three times for 12 h at 1100, 1150 and 1250 °C, respectively; these heating treatments were followed by a natural cooling step in the furnace. The composition $x=0.09$ was then synthesized. They were also characterized by powder XRD after quenching.

2.2. Quenching procedure

After synthesis, the pellets were held 2 h at the quenching temperature and then thrown in liquid N_2. The quenching temperature lies in the 1200–1500 °C range.

2.3. Preparation of the samples for in situ high temperature XRD

It has been previously reported that firing at 1350 °C for 6 h could lead to Li loss and to an increase of the La content in the compound [17,20]. Therefore, the samples used for in situ high temperature X-ray powder diffraction measurements were heated only up to 1150 °C. The same procedure used for the previous $x=0.11$ samples (a) has been followed for this synthesis. The heating treatments were followed by a natural cooling step in the furnace. Two compositions with low ($x=0.06$) and high ($x=0.11$) Li^+ contents were prepared.

2.4. Characterization of the samples

The samples were characterized by powder XRD at room temperature on a D5000 Siemens diffractometer (radiation CuKα; 2θ range = 9–129°; step $\Delta 2\theta = 0.04°$; time by step = 18 s), and for in situ high temperature experiments on Philips PW1810 diffractometer equipped with high temperature Anton Paar chamber, same 2θ range, step $\Delta 2\theta = 0.02°$; time by step = 1 s. The powder sample was heated from RT to 500 °C and then up to 1200 °C by step of 100 °C. The heating rate was 50 °C min^{-1}. From 500 to 1200 °C, the sample was kept 20 min at a given temperature before X-ray data acquisition and further heating. In all cases, the diffraction patterns were analyzed through the Rietveld method by the FULLPROF program [39]. The problem of the broadening of the superstructure lines was overcome as described in Ref. [5].

The total conductivity measurements were performed in the −125 to +25 °C temperature range. Complex impedance spectroscopy was carried out in the 10 MHz–1 Hz frequency range, with a 400-mV (r.m.s.) applied voltage, using a Solartron 1260 Impedance Gain Phase Analyser as described previously [17].

3. Results and discussion

3.1. Quenched samples

3.1.1. X-ray diffraction patterns analysis

Fig. 2 shows typical XRD patterns of LLTO ($x = 0.09$) as prepared (top) and after (bottom) quenching at 1400 °C. A broadening of the superstructure lines (marked with asterisks) is clearly observed. Despite the high temperature used for quenching, we did not succeed in obtaining, by this way, completely flat X-ray diffractograms at the 2θ positions where the superstructure lines appear. Such broadening has already been observed when Li^+ content (or x) decreases [5]. This is explained by an unequal distribution of La^{3+} ions between La1 and La2 positions and the formation of antiphase domains that creates a disordered situation in the regular sequence …La1–La2–La1… along the c-axis [5].

A Rietveld analysis of the XRD patterns has been performed on samples after synthesis and after quenching to determine the cell parameters and the La^{3+} populations in La1 and La2 positions as a function of the quenched temperature. Fig. 3 shows the good agreement obtained between the measured

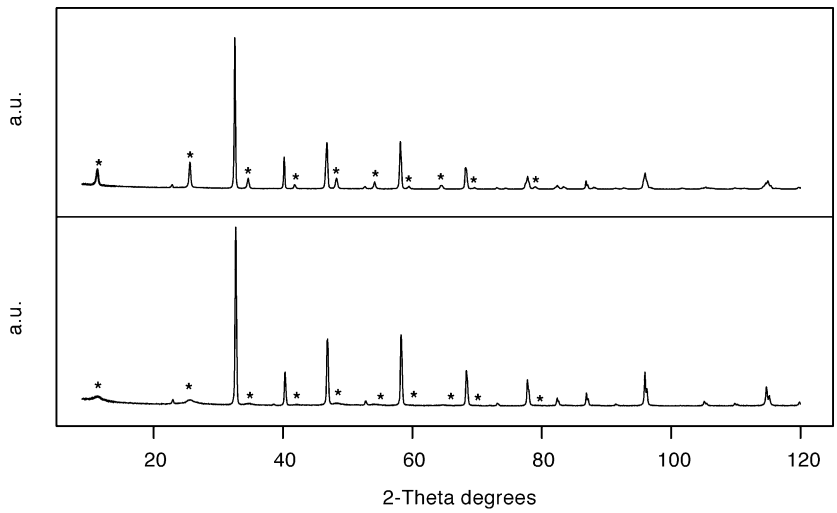

Fig. 2. Experimental X-ray diffractograms for $x = 0.09$ sample. Top: as-prepared compound; bottom: after quenching at 1400 °C. The asterisks show the superstructure lines (hkl with $l = 2n + 1$).

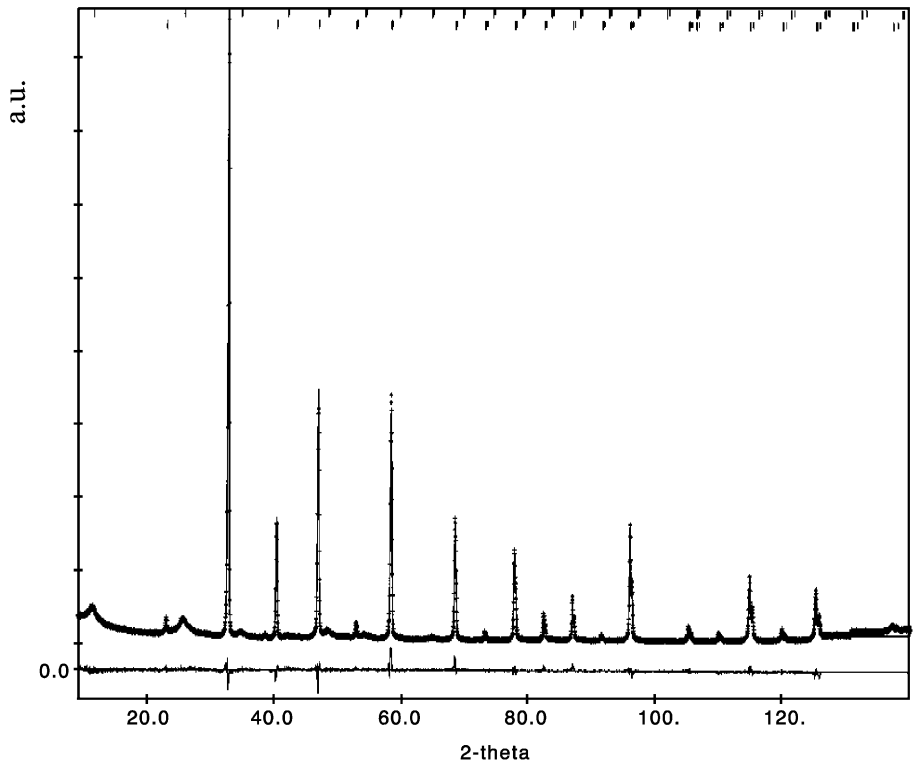

Fig. 3. Calculated and observed (· · ·) X-ray diffractograms for $x = 0.09$ sample quenched at 1400 °C. The difference spectrum is shown below at the same scale. The broad superstructure lines (*hkl* with $l = 2n + 1$) are treated as those belonging to a "second phase" [5]. Reliability factors: Rp = 13.3, Rwp = 13.4; for the narrow lines "phase 2", Bragg *R*-factor = 4.98; for the superstructure lines "phase 1", Bragg *R*-factor = 21.8; B_{eq} (in Å^2): La1 = 0.29(11), La2 = – 0.81(45), Ti = – 0.24(12), for all O = 2.48(8).

and calculated patterns for a sample quenched at 1400 °C. As previously explained in Ref. [5] and to overcome the problem of the broadening of the superstructure lines as *x* decreases, we used for the pattern refinement the "two phases" option of the Fullprof software [39], although the oxide is a one-phase compound. The superstructure lines of the pattern refer to "one phase" and the other lines to the "second phase", the atomic model being the same in both "phases". The use of the "multi-phase" option of the software is shown as small bars in Fig. 3 (top). The goodness of this procedure is evaluated from the difference spectrum drawn at the bottom of Fig. 3 and from the reliability factors obtained after refinement. We can then refine simultaneously, without correlation problems, the anisotropic thermal parameters of La^{3+} and its occupancy.

Fig. 4 shows the variation of the cell parameters: $a = b$ and $c/2$ as a function of the quenching temperature for the two samples $x = 0.09$ and $x = 0.11$. Fig. 5 presents the evolution of the La^{3+} populations of the La1 and La2 sites (in % occupancy of each site with La^{3+} ions) versus the quenching temperature for both compositions. The errors on the La^{3+} % occupancies are estimated to be three times the estimated standard deviation (e.s.d.) calculated by the Fullprof software. In all cases, they were found to be smaller than 0.5%. Before quenching, the cell parameters and La^{3+} % occupancy of the La1 and La2 sites agree with previous values obtained on this composition [5]. Particularly, the occurrence of the tetragonal distortion ($c/2a$) of the cubic cell is clearly seen for the compound with low Li^+ content ($x = 0.09$). As for the corresponding cell parameters with quenching for both compounds, very slight changes can be observed

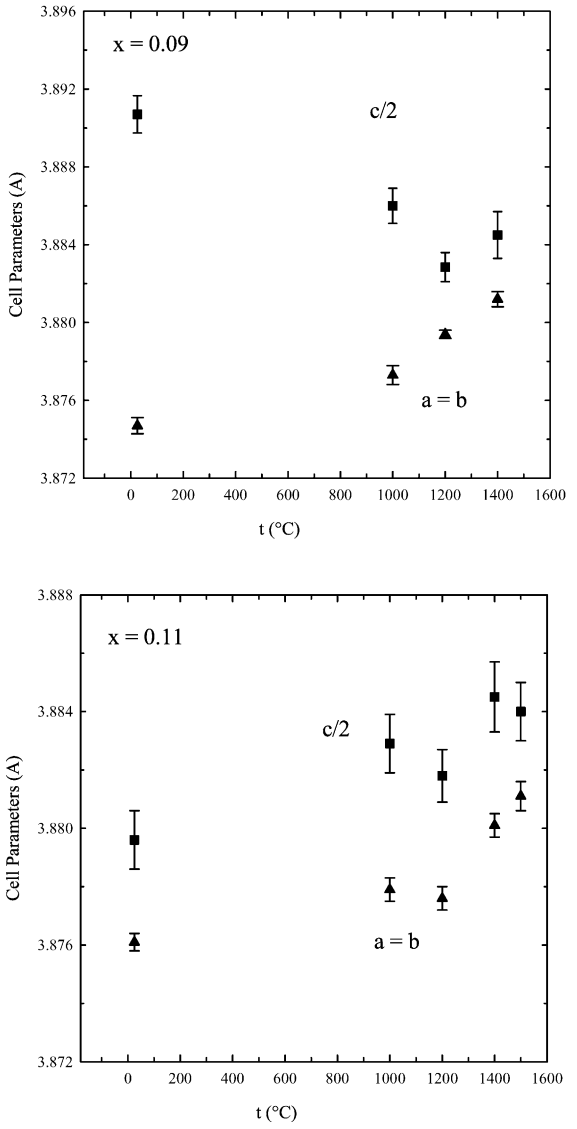

Fig. 4. Unit cell parameters (in Å) for $x=0.09$ and $x=0.11$ samples versus quenching temperature. (▲: $a=b$, ■: $c/2$).

for the populations. It has to be noticed that the same experiment performed with compounds with higher x value ($x=0.12$) did not lead to the formation of a cubic phase (the superstructure lines are broad, but they are always present). This result rules out a possible composition influence on the cubic phase formation. We suppose that the impossibility to form the cubic phase is due to a very fast reordering of the La^{3+} ions during quenching. On the contrary, Harada et al. [11] seem to have reached the cubic form (for $x=0.11$) by a more efficient quenching process. Interestingly, in that paper, the authors discussed the thermodynamically controlled extent of the La^{3+} ordering that can be reversibly changed by annealing the cubic samples in the 600–1150 °C temperature range. This result suggests that thermal diffusion of

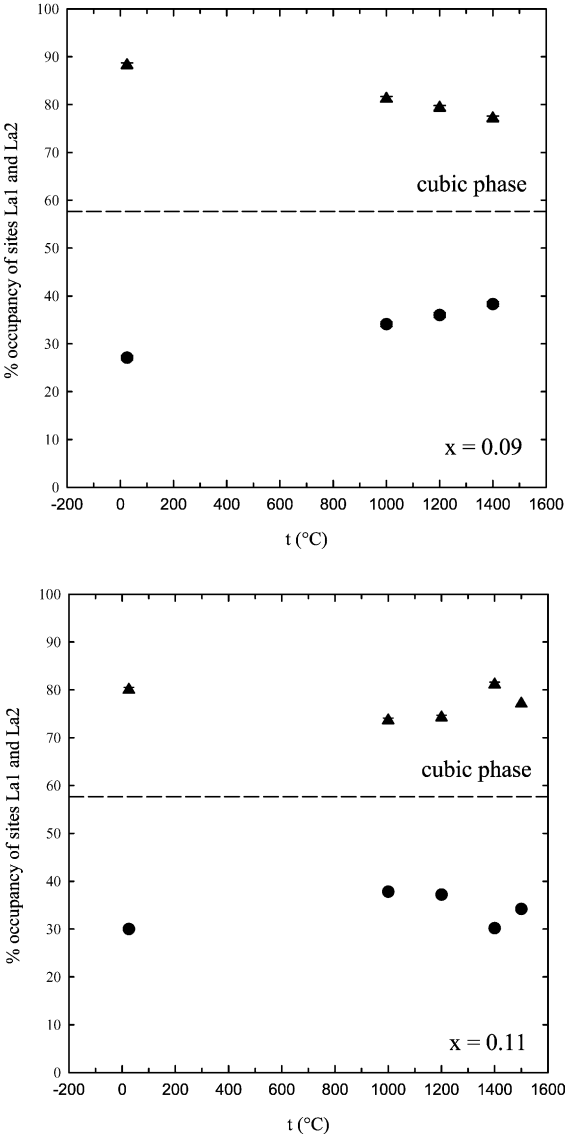

Fig. 5. % La^{3+} occupancy of the La1 (●) and La2 (▲) sites versus quenching temperature for $x=0.09$ and $x=0.11$ samples after quenching.

La^{3+} ions can occur in these compounds. Furthermore, this work pointed out the necessity to work with really equilibrated samples, i.e. with well-fixed La1 and La2 populations.

3.1.2. Conductivity measurements

The total conductivity (electronic and ionic) was checked on $x=0.09$ samples by impedance spectroscopy in the -125 to $+25$ °C temperature range before and after quenching at 1200 °C. In a previous paper, we have shown that the electronic conductivity is very small ($\sigma_e = 5 \times 10^{-10}$ S cm^{-1} at 25 °C [17]) in these solid solution compounds. Therefore, the conductivity is mainly ionic. The analysis of the impedance spectroscopy data has been made with the Complex Nonlinear Least Squares (CNLS) fitting procedure of Solartron. This procedure allows us to determine the bulk conductivity of our samples from the data that also contain grain boundary and electrode interfaces contributions. The activation energy of the bulk conductivity decreases very slightly with quenching, from 0.28 to 0.26 eV, and the bulk conductivity remains the same at room temperature ($\approx 5 \times 10^{-4}$ S cm^{-1}), confirming that quenching has a very small effect on the structure of the compound and consequently on its electrical properties. On the other hand, Harada et al. [11] observed a significant change in the bulk conductivity for the ordered (tetragonal) and completely disordered (cubic) $x=0.11$ samples: 6.88×10^{-4} and 1.53×10^{-3} S cm^{-1}, respectively, at room temperature, associated to a slight decrease of the activation energy from 0.34 to 0.32 eV, respectively.

3.2. In situ X-ray thermodiffractometry experiments

In order to check our hypothesis of a very fast reordering of La^{3+} ions during quenching, we made some in situ X-ray thermodiffractometry experiments on $x=0.06$ and $x=0.11$ samples prepared at the highest temperature of 1150 °C to prevent lithium loss, as explained in the experimental part of this paper.

Figs. 6 and 7 present the evolution of the cell parameters and the La^{3+} ions' %occupancy of La1 and La2 sites, respectively, as a function of temperature for $x=0.06$ and $x=0.11$ compounds. These values have been obtained from the classical Rietveld refinement of the high temperature XRD (HT-XRD) data. These data have been collected with a low counting time per step (1 s). The experimental setup imposes this low counting time. Before analysing the results, we carefully checked if such a low counting time did not greatly influence the results of our refinements. To do so, we compared at room temperature the results obtained with this procedure with the

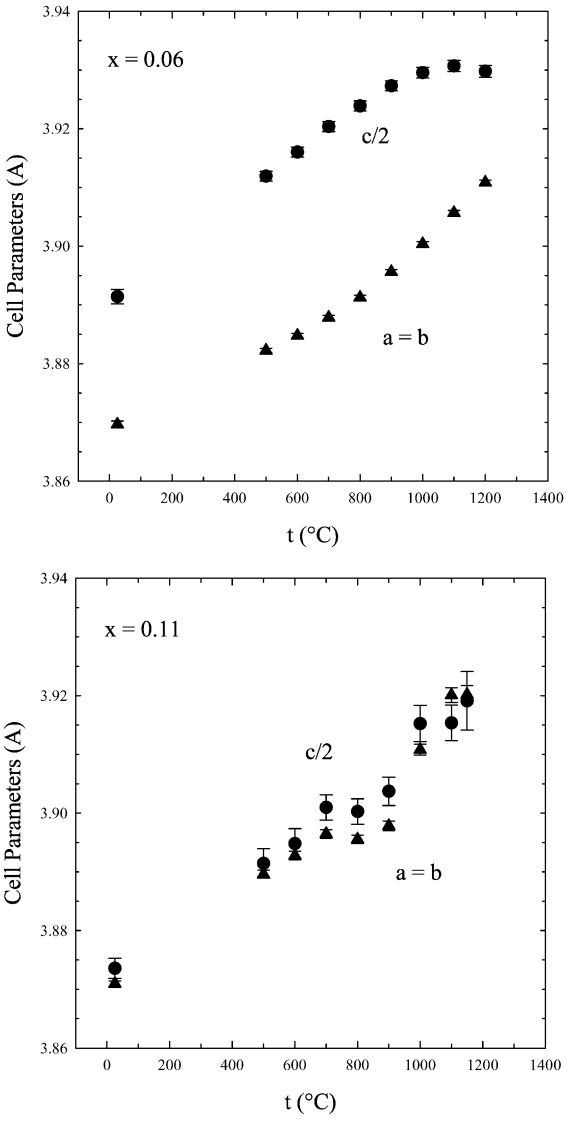

Fig. 6. Unit cell parameters (in Å) versus temperature, obtained from in situ X-ray thermodiffractometry experiments, for $x=0.06$ and $x=0.11$ samples versus temperature (▲: $a=b$, ●: $c/2$).

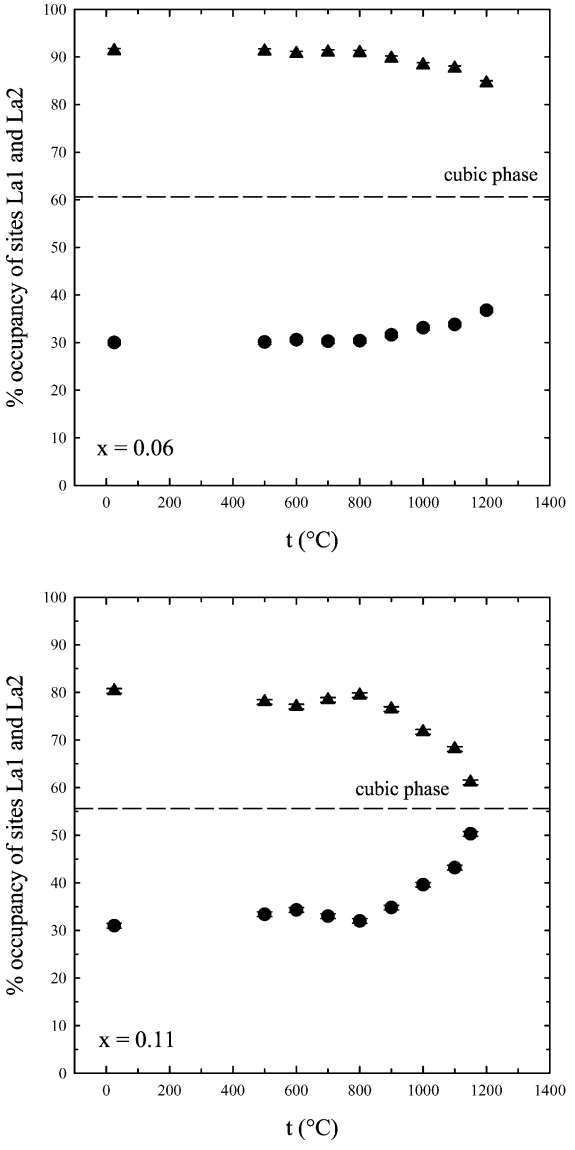

Fig. 7. La^{3+} % occupancy of the La1 (●) and La2 (▲) sites versus temperature, obtained from in situ X-ray thermodiffractometry experiments, for $x=0.06$ and $x=0.11$ samples. Typical reliability factors: Rp = 21.4, Rwp = 25.2; for the narrow lines or "phase 2", Bragg R-factor = 11.1; for the superstructure lines or "phase 1", Bragg R-factor = 18.7.

previous results obtained with a higher counting time. It can be seen in Fig. 6 that the cell parameters are in good agreement with those obtained in Ref. [5] and in Fig. 4 for $x=0.09$ where a counting time of 18 s is used. The same remark can be made for the La^{3+} ions' % occupancy. This is not surprising if we consider the fact that La^{3+} ions are the heaviest X-ray scatterers in LLTO.

Fig. 6 shows, as previously observed, that the tetragonal distortion $c/2a$ vanishes for high Li^{+} content (or high x). Furthermore, as temperature increases, the cell parameters increase for both compositions. This situation is very different from that observed on a quenched sample (see Fig. 4), confirming the poor efficiency of our quenching process. It also reveals that a transition observed in the $x=0.11$ compound begins around 800 °C (Fig. 6). This temperature was also noticed by Harada et al. [11]; they show that the La^{3+} reordering in $x=0.11$ quenched LLTO samples is very fast above 900 °C and becomes very sluggish below 800 °C [11].

Fig. 7 shows that the thermal diffusion of the La^{3+} ions (or disordering) begins clearly above 800 °C for both compounds. This observation is also evidenced in Fig. 8 that presents the plot of the $I_{001}/(I_{102}+I_{110})$ ratio versus temperature for the $x=0.11$ compound. I_{001} is the observed diffracted intensity corresponding to the strongest superstructure line (hkl with $l=2n+1$) and $(I_{102}+I_{110})$ is the sum of the two observed diffracted intensities that are the components of the

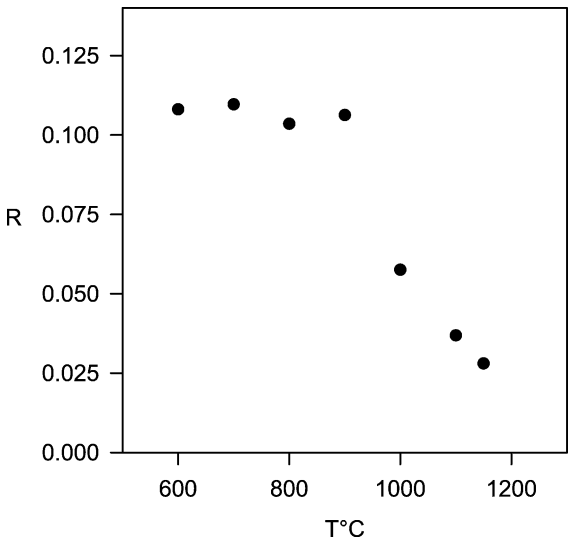

Fig. 8. $R=I_{001}/(I_{102}+I_{110})$ ratio versus temperature, obtained from in situ X-ray thermodiffractometry experiments ($x=0.11$).

diffraction pattern's strongest line. However, the disordering depends on the composition. For low Li^+ content, the disordering remains limited, even at 1200 °C (Fig. 7, $x=0.06$), whereas for high Li^+ content, an almost cubic phase is formed by in situ heat treatment at 1200 °C (Fig. 7, $x=0.11$). Unfortunately, quenching cannot retain this disordering, suggesting a very fast process of reordering occurs in these materials. Furthermore, it seems that an easy thermal disordering of the La^{3+} ions—and concomitantly their very fast reordering after quenching—are strongly favoured for samples with a $c/2a$ distortion ratio very close to 1. In other words, high Li^+ content and/or low La^{3+} content favours this disordering/ordering process.

4. Conclusion

In this study, the thermal ordering/disordering of La^{3+} ions between two unequivalent positions (La1 and La2) in the structure of the fast ionic conductor $La_{2/3-x}Li_{3x}TiO_3$ perovskite (space group $P4/mmm$) has been evidenced by X-ray examinations on quenched and in situ heated samples. In this structure, where fast lithium conduction occurs, La^{3+} thermal diffusion becomes noticeable above 800 °C, most likely along the quadratic bottlenecks of oxide ions between La1 and La2 perovskite cages. Structural and compositional factors noticeably affect the La^{3+} thermal diffusion, as demonstrated by the two compositions examined, a lanthanum-poor one ($x=0.11$) and a lanthanum-rich one ($x=0.06$), the former showing higher thermal diffusivity of La^{3+}. A key factor could be the sterical hindrance due to oxygen bottlenecks, which in turn is revealed by the $c/2a$ distortion ratio: if it is very close to 1 (as for $x=0.11$ composition), the La^{3+} ions diffusivity between La1 and La2 is likely to be favoured. Furthermore, a high density of La^{3+} ions tends to impair diffusivity itself. For both the above converging reasons, $x=0.11$ composition reaches a nearly complete disordering of La^{3+} ions at 1200 °C, the temperature at which the cubic form is nearly reached. The kinetics of the fast La^{3+} ions disordering/ordering in the temperature range 900–1200 °C as here evidenced has to be fully considered during the preparation of samples of the LLTO family, as thermal history can noticeably change La^{3+} partition and consequently influence both the conductivity and the structural characteristics of the prepared phase. For the above reasons, completely equilibrated samples must be obtained by proper heating times at temperatures higher than 800 °C.

References

[1] A.G. Belous, G.N. Novitskaya, S.V. Polyanetskaya, Yu.I. Gornikov, Russ. J. Inorg. Chem. 32 (1987) 156.
[2] Y. Inaguma, C. Liquan, M. Itoh, T. Nakamura, T. Uchida, H. Wakihara, M. Wakihara, Solid State Commun. 86 (1993) 689.
[3] H. Kawai, J. Kuwano, J. Electrochem. Soc. 141 (1994) L78.
[4] A.D. Robertson, S. Garcia-Martin, A. Coats, A.R. West, J. Mater. Chem. 5 (1995) 1405.
[5] J.-L. Fourquet, H. Duroy, M.-P. Crosnier-Lopez, J. Solid State Chem. 127 (1996) 283.
[6] J. Ibarra, A. Varez, C. Leon, J. Santamaria, L.M. Torres-Martinez, J. Sanz, Solid State Ion. 134 (2000) 249.
[7] A. Varez, F. Garcia-Alvarado, E. Moran, M.A. Alario-Franco, J. Solid State Chem. 118 (1995) 78.
[8] J.A. Alonso, J. Sanz, J. Santamaria, C. Leon, A. Varez, M.T. Fernandez-Diaz, Angew. Chem., Int. Ed. Engl. 39 (2000) 619.
[9] Y. Inaguma, T. Katsumata, J. Yu, M. Itoh, Mater. Res. Soc. Symp. Proc. 453 (1997) 623.
[10] Y. Harada, T. Ishigaki, H. Kawai, J. Kuwano, Solid State Ion. 108 (1998) 407.
[11] Y. Harada, Y. Hirakoso, H. Kawai, J. Kuwano, Solid State Ion. 121 (1999) 245.
[12] Y. Hirakoso, Y. Harada, J. Kuwano, Y. Saito, Y. Ishikawa, T. Eguchi, Key Eng. Mater. 169–170 (1999) 209.
[13] Y. Inaguma, J. Yu, Y.-J. Shan, M. Itoh, T. Nakamura, J. Electrochem. Soc. 142 (1995) L8.
[14] J.M.S. Skakle, G.C. Mather, M. Morales, R.I. Smith, A.R. West, J. Mater. Chem. 5 (1995) 1807.
[15] Y.J. Shan, Y. Inaguma, M. Itoh, Solid State Ion. 79 (1995) 245.
[16] A.G. Belous, Solid State Ion. 90 (1996) 193.
[17] O. Bohnke, C. Bohnke, J.-L. Fourquet, Solid State Ion. 91 (1996) 21.
[18] K.M. Nairn, M. Forsyth, M. Greville, D.R. MacFarlane, M.E. Smith, Solid State Ion. 86 (1996) 1397.
[19] Y. Inaguma, Y. Matsui, J. Yu, Y.-J. Shan, T. Nakamura, M. Itoh, J. Phys. Chem. Solids 58 (1997) 843.
[20] J. Emery, J.-Y. Buzaré, O. Bohnke, J.-L. Fourquet, Solid State Ion. 99 (1997) 41.
[21] Y. Inaguma, J. Yu, T. Katsumata, M. Itoh, J. Ceram. Soc. Jpn., Int. Ed. 105 (1997) 548.
[22] C. Leon, J. Santamaria, M.A. Paris, J. Sanz, J. Ibarra, L.M. Torres, Phys. Rev., B 56 (1997) 5302.
[23] J.-S. Lee, K.S. Yoo, T.S. Kim, H.J. Jung, Solid State Ion. 98 (1997) 15.
[24] O. Bohnke, J. Emery, A. Veron, J.-L. Fourquet, J.-Y. Buzaré, P. Florian, D. Massiot, Solid State Ion. 109 (1998) 25.
[25] N.S.P. Bhuvanesh, O. Bohnke, H. Duroy, M.-P. Crosnier-Lopez, J. Emery, J.-L. Fourquet, Mater. Res. Bull. 33 (1998) 1681.

[26] J. Emery, O. Bohnke, J.-L. Fourquet, J.-Y. Buzaré, P. Florian, D. Massiot, J. Phys., Condens. Matter 11 (1999) 10401.
[27] T. Katsumata, Y. Inaguma, M. Itoh, K. Kawamura, J. Ceram. Soc. Jpn., Int. Ed. 107 (1999) 615.
[28] Y. Harada, H. Watanabe, J. Kuwano, Y. Saito, J. Power Sources 81–82 (1999) 777.
[29] K.L. Ngai, C. Leon, Phys. Rev., B 60 (1999) 9396.
[30] H.-T. Chung, D.-S. Cheong, Solid State Ion. 120 (1999) 197.
[31] S. Kunugi, Y. Inaguma, M. Itoh, Solid State Ion. 122 (1999) 35.
[32] A.I. Ruiz, M.L. Lopez, M.L. Veiga, C. Pico, J. Solid State Chem. 148 (1999) 329.
[33] K.L. Ngai, C. Leon, Solid State Ion. 125 (1999) 81.
[34] A. Varez, M.L. Sanjuan, M.A. Laguna, J.I. Pena, J. Sanz, G.F. de la Fuente, J. Mater. Chem. 10 (2000) 1.
[35] M.A. Paris, J. Sanz, C. Leon, J. Santamaria, J. Ibarra, A. Varez, Chem. Mater. 12 (2000) 1694.
[36] M. Abe, K. Uchino, Mater. Res. Bull. 9 (1974) 147.
[37] D. Mazza, S. Ronchetti, O. Bohnké, H. Duroy, J.L. Fourquet, Solid State Ion. 149 (2002) 81.
[38] N.E. Brese, M. O'Keeffe, Acta Crystallogr., B 47 (1991) 192.
[39] J. Rodriguez Carjaval, FULLPROF Software: Rietveld Pattern Matching Analysis of Powder Patterns, ILL, Grenoble, 1990.